European Journal of Chemistry

View Journal Online
View Article Online

# Basicity determination of SBA-15 doped with different alkaline metals through $CO_2$ adsorption and isopropanol decomposition

Natalia Romina Reale and María Virginia Cagnoli *

*Departamento de Ingeniería Química, Facultad de Ingeniería, Universidad Nacional de La Plata, Centro de Investigación y Desarrollo en Ciencias Aplicadas, Consejo Nacional de Investigaciones Científicas y Técnicas, Calle 47, Nº. 257, 1900, La Plata, Argentina*
natyreale@gmail.com (N.R.R.), mavic@quimica.unlp.edu.ar (M.V.C.)

** Corresponding author at: Departamento de Ingeniería Química, Facultad de Ingeniería, Universidad Nacional de La Plata, Centro de Investigación y Desarrollo en Ciencias Aplicadas, Consejo Nacional de Investigaciones Científicas y Técnicas, Calle 47, Nº. 257, 1900, La Plata, Argentina.*
*e-mail: mavic@quimica.unlp.edu.ar (M.V. Cagnoli).*

RESEARCH ARTICLE

10.5155/eurjchem.11.2.100-104.1960

Received: 03 January 2020
Received in revised form: 05 March 2020
Accepted: 09 March 2020
Published online: 30 June 2020
Printed: 30 June 2020

KEYWORDS

SBA-15
Supported iron
Alkaline cations
CO decomposition
Isopropanol reaction
Fischer-Tropsch synthesis

ABSTRACT

In order to increase the activity and selectivity towards to light olefins in the Fischer-Tropsch synthesis, new support for the role of iron (Fe) are presented. Thus, SBA-15 was synthetized and doped with different alkaline metals preserving the structural characteristics of the mesoporous solid. The samples were characterized by X-ray diffraction at low angles, $N_2$ adsorption, atomic absorption spectroscopy, $CO_2$ desorption at programmed temperature and isopropanol test. The alkaline metals (Li, K and Cs) introduction into the channels of the solid, generate basic sites of different strength that are not present in the SBA-15 without doping and do not produce significant changes in the structural and textural properties of the SBA-15, only a densification in the walls of the channels is evidenced. According to the alkaline metal used and through $CO_2$ adsorption and isopropanol decomposition, it was possible to established the order by the total number of sites: Li >> K ≈ Cs, and the force order for both types of sites (weak and intermediate): Li > Cs > K.

**Cite this**: *Eur. J. Chem.* **2020**, *11(2)*, 100-104 **Journal website**: www.eurjchem.com

## 1. Introduction

The Fischer-Tropsch Synthesis (FTS) is an industrial process used to produce hydrocarbons from synthesis gas (mixture of $H_2$ and CO) [1]. Different metals are active as catalysts in FTS, although cobalt (Co) and Fe are the most commonly used for this process [2]. Precipitated or bulk Fe catalysts are preferred over Co catalysts, since, among other things, they are more selective towards alkenes. On the other hand, the use of supported metal catalysts in the FTS has been deeply studied in recent years [3,4]. However, a supported catalyst, selective to light olefins and with acceptable activity, is a subject that has not been resolved yet. These catalysts should have a narrow crystal size distribution, essential condition to increase the catalyst selectivity [5] and an adequate basicity, which not only favors the selectivity to the olefins production, but also increases the catalyst activity [6,7]. One way to obtain a narrow Fe crystal size distribution is to locate the Fe crystals within the channels of the mesoporous solid. The mesoporous solid SBA-15 seems to meet all these conditions since it has a narrow crystal size distribution, with hexagonal arrangement [8], structural properties that indicate that the SBA-15 is an appropriate solid to carry out the support requirements, since if the iron enters inside the channels, a narrow size distribution will be obtained in the desired range. On the other hand, the high wall thickness that this solid presents, gives it a high thermal and hydrothermal stability that allows carry out all the preparatory steps. The alkali metals have been extensively studied as promoters to increase the activity and selectivity in the CO hydrogenation, furthermore in contact with a transition metal can alter the binding energies and the adsorption capacity of the molecules [9]. According to Lee and Ponec [10] the rate of CO dissociation and the dispersion of the active metal on the support are increased by the presence of an alkaline promoter. Alkali metals of the first group of the periodic table, such as: Li, Na, K, Rb and Cs are the most used as promoters in the FTS [11]. Three alkaline cations (Li, K and Cs) were chosen with the purpose of giving a different promoter effect to the iron catalyst. Therefore, we present the synthesis and characterization of three modified mesoporous supports Li-SBA-15, K-SBA-15 and Cs-SBA-15, which will be potentially used in the FTS.

The aim of the present work is to prepare new supports for iron, promoted with alkaline metals, and characterized them through $CO_2$ decomposition and isopropanol reaction, in



http://dx.doi.org/10.5155/eurjchem.11.2.100-104.1960

**Table 1.** Specific surface between 400 and 700 $m^2/g$, pore volumes between 0.6 and 1.0 $cm^3$ and pore radii close to 40 Å.

| Sample | $S_g$ ($m^2/g$) | $V_p$ ($cm^3/g$) | $r_p$ (Å) | t (Å) |
|---|---|---|---|---|
| SBA-15 | 893 | 1.09 | 41 | 68 |
| Li-SBA-15 | 653 | 0.98 | 40 | 23 |
| K-SBA-15 | 529 | 0.75 | 41 | 21 |
| Cs-SBA-15 | 435 | 0.61 | 35 | 28 |

order to use them in the Fischer-Tropsch synthesis to increase the activity and selectivity trough light olefins.

## 2. Experimental

### *2.1. Sample preparation*

SBA-15 support was synthesized according to references [8,12] using tribloque Pluronic P123 copolymer (EO20-PO70-EO20) as structure directing agent and tetraethylorthosilicate (TEOS) as a source of silicon. Pluronic P123 (12 g) was dissolved in water (360 mL) and HCl solution (60 mL, 37%, *w*:*w*) with stirring during 3 h at 313 K. Then, TEOS (27 mL) was added, and the solution was kept stirring for 24 h at 313. The mixture was aged overnight at 363 K, without stirring. The solid was recovered by filtration, washed, and dried in air at room temperature (RT). Calcination in air was carried out from RT to 773 K at 1 K/min and kept at 773 K for 6 h. SBA-15 modified with alkali metals was prepared using the same methodology described above. The only difference was that the $CsNO_3$ or $KNO_3$ or the $LiNO_3$ were added with P123 and the final solid was not recovered by filtration and washed. The remaining water in the gel of synthesis was removed by evaporation at 333 K under vacuum. The amount of alkali metal in each case was calculated in function of maintaining an atomic ratio M/Si = 0.0125. Thus, every 12 g of P123 we added 0.102 g of $LiNO_3$ or 0.15 g of $KNO_3$ or 0.295 g of $CsNO_3$. The solids were named Li-SBA-15, K-SBA-15 and Cs-SBA-15.

### *2.2. Characterization of the samples*

The samples were characterized by X-ray diffraction (XRD) at low angles, $N_2$ adsorption (BET), atomic absorption spectroscopy, $CO_2$ programmed temperature desorption (TPD) and isopropanol test. X-ray diffraction was carried out in a Shimadzu equipment, model XD3A, using Cu Kα radiation at 40 kV and 40 mA in the range of 2θ = 0.5-4.0° with steps of 0.020 counting time of 2 s/step. The textural properties, specific surface area (Sg), specific pore volume (Vp) and pore diameter (Dp), were measured in a computer Micromeritics ASAP 2020 V1.02 E. The alkali metal content of the solids was determined by absorption in a Model IL 457 AA/AE spectrophotometer equipment from Instrumentation Laboratory Inc. The samples were attacked with HCl and HF mixture until complete dissolution and then treated according to conventional methods for this technique. The TPD-$CO_2$ analysis was carried out in a stainless-steel fixed bed reactor (2.54 cm o.d.). The samples were activated in Ar current (20 $cm^3$/min) at 973 K for 2 h. Then a $CO_2$/Ar (8:100, *v*:*v*) stream was passed through the sample for 5 minutes and was purged with pure Ar to remove $CO_2$. After this, the solid was heated in Ar current with a heating rate of 10 K/min up to 973 K with the purpose of desorbing the $CO_2$. This gas stream was mixed with $H_2$ stream (20 $cm^3$/min) and passed through $Ni/SiO_2$ catalyst at 673 K to convert the $CO_2$ to $CH_4$ which was quantified using the flame ionization detector (FID) detector. In this way, the amount of $CO_2$ absorbed was determined. Among the most studied reactions, the isopropanol decomposition seems to be one of the most useful to investigate the acid-base properties of the catalytic sites of metal oxides. Thus, the catalysts can be classified according to their tendency to produce dehydration or dehydrogenation of isopropanol to propene or acetone respectively. In this way, the isopropanol decomposition reaction was used for the evaluation of the weak and/or basic acid sites of the supported solids on SBA-15, for which experimental laboratory equipment was prepared.

## 3. Results and discussion

The porous hexagonal structure of the solid SBA-15 has a characteristic diagram code XRD at low angles. According to the literature, there are three lines of diffraction at 2θ = 0.9, 1.6 and 1.80° corresponding to the planes (100), (110) and (200), associated with the hexagonal symmetry of the SBA-15 [8]. The X-ray diffractogram at low angles of the SBA-15 and the impregnated supports Li-SBA-15, K-SBA-15 and Cs-SBA-15 are shown in Figure 1.

The three descriptive lines above can be clearly distinguished in the X-ray diffractogram. The intensity of the first line (plane 100) gives idea of the high symmetry of the obtained solids, and the presence of two peaks at high angles shows a high frequency in the structure. The positions of the diffraction peaks are coincident, with very slight differences, with those published in the literature which shows that there are no major changes in the solid structure after incorporating the alkaline metals.

Only in doped SBA-15 solids, the position of the most intense peak shows a slight shift towards larger angles compared to the un-doped solid. Taking into account the position of the peak in the plane 100 is inversely related to the interplanar distance. It is concluded that the introduction of the alkaline metals produces the contraction of the structure. Other authors have reported similar results [13].

The $N_2$ adsorption-desorption results of the synthesized solids denote type IV isotherms, characteristics of mesoporous solids with a narrow pore diameter distribution, as it was demonstrated in a previous paper [7]. In addition, all solids exhibit H1 hysteresis type, which is characteristic of mesoporous materials with uniform pore size and shape. The strong increase in $N_2$ adsorption to approximately saturation and the slight distortion in the values of the hysteresis loop (most notable for the case of Li-SBA-15) would presume a slight tendency of the H1 hysteresis type towards to H3 hysteresis type [14]. However, in the three doped solids no significant differences are observed with respect to the un-doped solids, thus it can be indicated that the amount of alkaline metals has no consequences on the shape of the pores and their narrow pore size distribution. From BET isotherms, the values of the specific surface area (Sg), pore volume (Vp), pore radius (rp) and wall thickness (t) of the channels can be calculated.

Table 1 shows the values of the specific surface area between 400 and 700 $m^2/g$, pore volumes between 0.6 and 1.0 $cm^3$ and pore radii close to 40 Å, typical values for this type of mesoporous solid. Comparing the values obtained for the non-doped SBA-15 solid with respect to doping, it can be observed that the differences are not very large and are in the range of the expected values for these solids [12] The most important decrease in values of Sg and Vp are observed for Cs-SBA-15, perhaps due to the larger size of the alkaline cation. In addition, Table 1 displays that the pore radius values have not decreased in the same way as the specific volume and the specific surface area. This would indicate that when alkali metals are added, a partial filling of the channels occurs.

**Table 2.** Results obtained from the TPD-$CO_2$ essays of the supports *.

| Support | $-q_0$ in $M_2O$ | T (K) | W (K) | $A_2/A_1$ | $\mu moles_{tot}/g_{MA}$ | $D_M$ (%) | T (K) |
|---|---|---|---|---|---|---|---|
| Li-SBA-15 | 0.80 | 377-458 | 73-136 | 1.78 | 4509 | 3.0 | 377-458 |
| K-SBA-15 | 0.89 | 338-379 | 41-101 | 1.78 | 235 | 0.9 | 338-379 |
| Cs-SBA-15 | 0.94 | 346-448 | 69-114 | 0.49 | 27 | 0.4 | 346-448 |

* $-q_0$ = Partial negative load of oxygen in alkali metal oxides; T = Maximum temperature of the desorption peak, W = Width of the desorption peak at half its height; $A_2/A_1$ = Ratio of areas from the second to the first desorption peak, $\mu moles_{tot}/g_{MA}$ = Total micromoles of $CO_2$ absorbed per gram of alkali metal; $D_M$ (%) = Alkali metal dispersion.

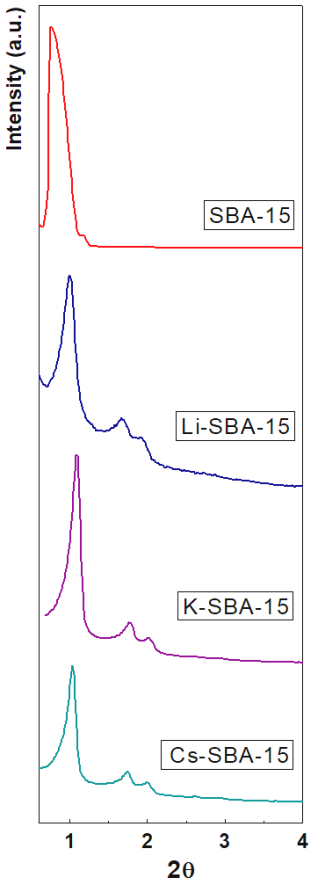


**Figure 1.** X-ray diffractogram at low angles of SBA-15 and the impregnated supports Li-SBA-15, K-SBA-15 and Cs-SBA-15.

On the other hand, the estimated wall thickness for the support is substantially less than that computed for the non-doped SBA-15. This is due to the contraction of the network parameters accompanied by a negligible change in the pore radius [13]. It is possible to speculate that the incorporation of the alkaline metal contracts the walls of the channels. Figure 2 shows the temperature desorption curves programmed for each doped support with the appropriate deconvolution using a least-squares non-linear fit with two Gaussian peaks.

It can be seen that the thermogram of the undoped SBA-15 solid does not present peaks of $CO_2$ desorption and its baseline was used to deduce from each diagram the doped supports. This denotes the absence of basic Lewis sites in un-doped solids, as reported in the literature [15]. The thermograms of the three doped supports have two peaks corresponding to the $CO_2$ desorption at relatively low temperatures in the range 340-380 and 380-460 K. These peaks correspond to $CO_2$ adsorbed in basic sites with different adsorption strength that will be called weak and intermediate strength sites. While, as mentioned, the un-doped SBA-15 does not possess any of those sites, they must be attributed to the presence of Group 1 alkaline metals of the periodic table located on the surface of the support, coinciding with previous reports [16].

In Table 2, it can be seen that the support with the most total basic surface sites per gram of alkali metal is Li-SBA-15, this amount is approximately 20 times higher than in K-SBA-15 and 170 times higher than in Cs-SBA-15. These results cannot be explained from the alkali metal mass content, since the contents of K and Cs are approximately 4 and 20 times greater than that of Li. The adsorption of $CO_2$ on alkaline or alkaline earth metals takes place under different species: bicarbonate, unidentate carbonates and bidentate carbonates [8-11].

The different types of adsorption reveal the different chemical nature of the oxygenated atoms. Thus, for the formation of unidentate carbonates, the presence of isolated $O^{-2}$ is necessary. This unidentate carbonates are usually present in edges and vertices of small crystals. Bidentate carbonates are formed on even Lewis acid/Brönsted base sites ($M^{n+}$-$O^{2-}$). Finally, the bicarbonate species are related to the surface hydroxyl species, which are the most labile of the three species. In general, the following order by force is proposed for the superficial basic sites: isolated $O^{2-}$ > pairs $M^{n+}$-$O^{2-}$ > OH groups. Although the total amount of $CO_2$ molecules is adsorbed on an alkali metal atom. Thus, if the total amount of $CO_2$ molecules adsorbed per gram of solid is related to the total number of alkali metal per gram of solid, an equivalent

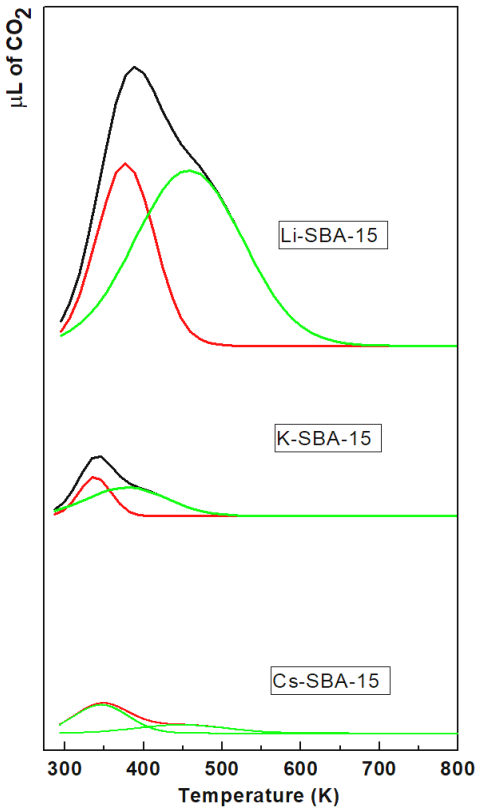


**Figure 2.** Desorption curves at programmed temperature for each doped support with the appropriate deconvolution, using a non-linear adjustment of least squares with two Gaussian peaks.

value to the dispersion could be obtained. This value would be independent of the amount of alkali metal added to the sample. In Table 2, it is observed that the sample Li-SBA-15 has a dispersion value three times greater than that of K-SBA-15 and 7 times higher than that of the sample of Cs-SBA-15.

These differences can be attributed to the greater degree of agglomeration of the species when the size of the alkaline cations is greater and/or to the increase of the number of alkaline ions located within the walls of the SBA-15 (which are inaccessible to the $CO_2$ molecules). The location of an alkali metal fraction within the walls of the SBA-15 is consistent with the network parameters and with the highest density of the doped SBA-15.

The maximum temperature and the width of the mid-height peak can be used for the purpose of obtaining the $CO_2$ desorption heat. An increase in those values indicates a greater heat of desorption and therefore a greater basic strength of the sites where the $CO_2$ has been adsorbed [13]. The surface oxides basicity is generally related to the electrical properties of the combined oxygen rings, so when the negative partial charge of these combined oxygen anions increases, the resulting oxide will be more basic.

In this sense, the negative partial load of oxygen ($-q_0$ in Table 2) would indicate the properties of the electrons, in oxides with a single component. These values $-q_0$ were calculated using the electronegativity equalization principle [14], a decrease of $-q_0$ can be observed when the atomic mass increases. However, comparing the three supports obtained in this work, in contrast with what is expected, it can be observed that the solid doped with Li has the highest basic strength for both weak and medium sites. Many authors [11,17] have found that Li generates stronger basic sites than expected, when it is used as a solid dopant.

K-SBA-15 sample has adsorbed 8 times more $CO_2$ per gram of metal charge than Cs-SBA-15; however, it has a metal content 5.4 times lower. In addition, both types of sites generated by K are weaker than those produced by Cs, since their desorption peaks are acute and appear at lower temperatures than those corresponding to Cs-SBA-15. These results have been reported by other authors [18].

Another result is that the samples Li-SBA-15 and K-SBA-15 have a population of sites of medium strength that is twice the population of weak sites (A2/A1 in Table 2), while in Cs-SBA-15 this situation is reversed.

In the present work it can be observed that although we generate superficial basic sites in the SBA-15 from the addition of alkaline metals, the structural properties of the support are maintained.

The sample which has the lower IPA molecules value at the exit (Figure 3), corresponds to that which has the greater IPA proportion converted to propene (no acetone has been detected). According to this criterion, the following basicity order is established: Cs-SBA15> K-SBA15, corroborating the order established so far by basic force of both types of sites: Cs> K. In this work, it can be observed that although we generate basic surface sites in SBA-15 from the addition of alkali metals, the structural properties of the support are maintained.

The order established from the isopropanol test corroborated the results obtained up to now resulting, by the total number of sites: Li >> K ≅ Cs and the order by basic force of both types of sites: Li > Cs > K.

## 4. Conclusions

SBA-15 was doped with different alkaline metals during synthesis, preserving the structural characteristics of the mesoporous solid.

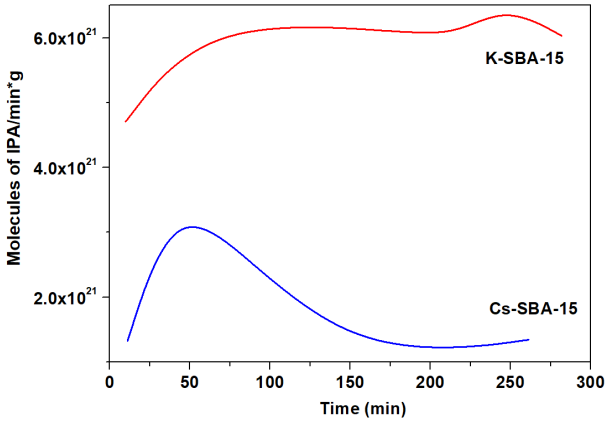


**Figure 3.** IPA molecules value vs. time.

The introduction of the alkaline metal inside the channels of the solid does not produce significant changes in the structural and textural properties of the SBA-15, only a densification in the walls of the channels is evidenced. The incorporation of alkaline metals in the support generates basic sites of weak and medium strength that are not present in the non-doped SBA 15. According to the alkaline metal used, the order established by the total number of sites is: Li >> K ≅ Cs, while the force order for both types of sites (weak and intermediate) is: Li > Cs > K.

## Disclosure statement

Conflict of interests: The authors declare that they have no conflict of interest.
Author contributions: All authors contributed equally to this work.
Ethical approval: All ethical guidelines have been adhered.
Sample availability: Samples of the compounds are available from the author.

## ORCID

Maria Virginia Cagnoli
http://orcid.org/0000-0003-3937-5558
Natalia Romina Reale
http://orcid.org/0000-0001-7759-1409

## References

[1]. Steynberg, A.; Fischer-Tropsch Technology, Steynberg, A.; Dry, M. (Eds.), *Stud. Surf. Sci. Catal.*, Elsevier, Amsterdam. **2004**, *152*, 1-63.
[2]. Luo, M.; Hamdeh, H.; Davis, B. *Catal. Today* **2009**, *140*, 127-134.
[3]. Vannice, M. *J. Catal.* **1975**, *37*, 449-461.
[4]. Bartholomew, C.; Recent Developments in Fischer-Tropsch Catalysis. Guczi, L. (Ed.). *Stud. Surf. Sci. Catal.*, Elsevier, Amsterdam, **1991**, *64*, 158-224.
[5]. Donald, M.; Storm, D.; Boudart, M. *J. Catal.* **1986**, *102*, 386-400.
[6]. Luo, M.; O'Brien, R.; Bao, S.; Davis, B. *Appl. Catal.* **2003**, *239*, 111-120.
[7]. Cano, L. A.; Cagnoli, M. V.; Bengoa, J. F.; Garcia-Fierro, J. L.; Marchetti. S. G. *J. Porous Mater.* **2016**, *24*, 631-638.
[8]. Zhao, D.; Huo, Q.; Feng, J.; Chmelka, B.; Stucky, G. *J. Am. Chem. Soc.* **1998**, *120*, 6024-6036.
[9]. Wang, C.; Xu, L.; Wang, Q. *J. Natural Gas Chem.* **2003**, *12*, 10-16.
[10]. van der Lee, G.; Ponec, V. *Catal. Rev. Sci. Eng.* **1987**, *29(2&3)*, 183-218.
[11]. Ngantsoue-Hoc, W.; Zhang, Y.; O'Brien, R.; Luo, M.; Davis, B. *Appl. Catal.* **2002**, *236*, 77-89.
[12]. Cano, L. A.; Cagnoli, M. V.; Bengoa, J. F.; Alvarez, A. M.; Marchetti, S. G. *J. Catal.* **2011**, *278*, 310-320.
[13]. Zhang, T.; Wang, R.; Geng, W.; Li, X.; Qi, Q.; He, Y.; Wang, S. *Sens. Actuators B Chem.* **2008**, *128*, 482-487.
[14]. Sing, K.; Everett, D.; Haul, R.; Moscou, L.; Pierotti, R.; Rouquerol, J.; Siemieniewska, T. *Pure Appl. Chem.* **1985**, *57*, 603-619.
[15]. Yang, S.; Zhu, W.; Zhang, Q.; Wang, Y. *J. Catal.* **2008**, *254*, 251-262.
[16]. Zhu, J.; Chun, Y.; Wang, Y.; Xu, Q. *Mat. Lett.* **1997**, *33*, 207-210.
[17]. Pawelec, B.; Castano, P.; Arandes, J.; Bilbao, J.; Thomas, S.; Pena, M.; Garcia, F. *J. Appl. Catal. A.* **2007**, *317*, 20-33.
[18]. Miyakoshi, A.; Ueno, A.; Ichikawa, M. *Appl. Catal. A* **2001**, *219*, 249-258.